Journal of Materials Science & Surface Engineering, 6(4): 837-844
ISSN (Online): 2348-8956; 10.jmsse/2348-8956/6-4.4

Theoretical Study of Spectral Responses of Homojonctions Based on $CuInSe_2$ Deposited on Substrate With or Without A Window Layer: Effect of An Electric Field

Y. Tabar · M. L. Sow · E. M. Keita · A. A. Correa · B. Mbow

Laboratory of Semiconductors and Solar Energy, Physics Department, Faculty of Science and Technology, University Cheikh Anta DIOP-Dakar-SENEGAL.

ABSTRACT

The aim of this work is to make a comparative study of the spectral response between the two models of solar cells, namely a homojonction deposited on substrate without a window layer: $CuInSe_2$(N)/ $CuInSe_2$(P) /CdTe(P^+) and a homojonction deposited on substrate with a window layer: CdS (N^+)/$CuInSe_2$(N)/ $CuInSe_2$(P)/CdTe(P^+). In this case we will calculate the respective different expressions of the spectral response by solving the continuity equations governing the variation of the minority carriers in each region for each model and using the boundary conditions. A simulation of this quantum efficiency with the energy is done, keeping the same values of geometrical parameters. The results show that the homojonction model with a window layer and deposited on substrate gives the best quantum efficiency. The window layer decreases the losses at the surface and at the window-emitter interface and increases in the base the collection of electrons. We will then study the influence of an internal electrical field due to a doping gradient on a homojonction deposited on substrate with or without a window layer. We note that the internal quantum efficiency rises with the increasing of the additional electric field in the window layer. We also note that the best quantum efficiency is obtained with a homojonction deposited on substrate for an internal electric field of $2.10^5 Vcm^{-1}$. We remark a concordance of our results to those found in literature.

ARTICLE HISTORY
Received 17-07-2018
Revised 10-09-2018
Accepted 26-09-2018
Published 26-11-2018

KEYWORDS
Thin films,
$CuInSe_2$,
CdS, CdTe,
Internal quantum efficiency,
Window layer and substrate effects,
Electric field

Introduction

The ternary compound $CuInSe_2$ (CIS) of the family I-III-VI_2 presented a considerable interest [1] in solar applications for some years [2-4]. This material is presently considered as the most promising because of its forbidden band (Eg= 1.04eV). Its higher absorption coefficient α (α=10^4-10^5 cm^{-1}) [5-6] allows it to absorb in a wide range of the solar spectrum, from the visible to the nearest infrared. It may also change the type of conduction (N or P) without doping foreign atoms [7].

However the conversion efficiency remains limited despite the good performance of this material. It is in order to improve the quantum efficiency that we will study a homojonction of $CuInSe_2$ with a CdS window layer. The whole things will be deposited on a CdTe substrate. The CdS window layer will be transparent in the incident radiation [8-9] and the substrate will return the uncollected carriers to the space charge region so that they can participate in the photocurrent.

The effect of an additional electric field due to the doping gradient on a homojonction deposited on a substrate with or without a window layer was also studied in this work.

Theoretical Study

Homojunction deposited on substrate $CuInSe_2$(N)/ $CuInSe_2$ (P) / CdTe (P^+)

Modelling

In order to simulate a homojunction model corresponding to an N-P junction deposited on a doped substrate P^+, we assume that the junction is between the two first layers and that the thickness of the substrate is infinitely large compared to the others geometrical parameters.

Figures 1 and 2 respectively represent the diagram and the band diagrams of a homojunction model N-P deposited on a P^+ type substrate. In Fig. 2: e_2, e_3 and e_4 respectively represent the thicknesses of the emitter, the base and the substrate and w represents the thickness of the space charge region. In figure 1 we have $x'_2 = e_2$, $x_3=e_2+ w + e_3$ and $H = e_2+ w + e_3+ e_4$.

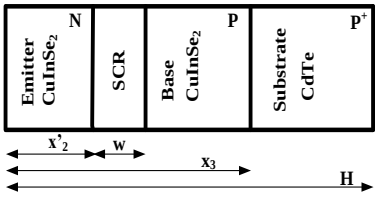

Figure 1: Diagram of the structure:$CuInSe_2$(N)/ $CuInSe_2$(P)/CdTe (P^+)

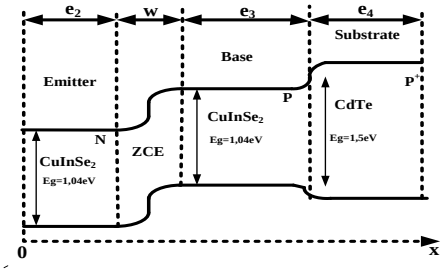

Figure 2: Energy band diagram of the structure: $CuInSe_2$ (N)/$CuInSe_2$(P)/CdTe (P^+)

Corresponding Author: Y Tabar, Tel: +221778943232
Email: yvesbadiath@hotmail.fr
Contents lists available at http://www.jmsse.org/ & http://www.jmsse.in/

Quantum efficiency in the emitter layer

The continuity equation governing the variation of the holes density in the N-type emitter under static mode is given by equation (1) [10-13]:

$$\frac{d^2\Delta p_2}{dx^2} - \frac{\Delta p_2}{Lp_2^2} + \frac{\alpha_2 \cdot N(1-R)e^{-\alpha_2 x}}{Dp_2} = 0 \qquad (1)$$

Where L_{p_2} is the diffusion length of the holes in the emitter [14], α_2 the absorption coefficient of $CuInSe_2$, Dp_2 the diffusion coefficient of the holes in the emitter, N: incident photon number and R: reflection coefficient.

The general solution of equation (1) is in the form:

$$\Delta p_2(x) = Ae^{x/Lp_2} + Be^{-x/Lp_2} + Ke^{-\alpha_2 x}$$

with $$K = -\frac{\alpha_2 N(1-R)Lp_2^2}{Dp_2(\alpha_2^2 \cdot Lp_2 - 1)}$$

The constants A and B were determined from the boundary conditions given by equations (2) and (3) [10-12]:

$$Dp_2 \frac{d\Delta p_2}{dx} = Sp_2 \cdot \Delta p_2 \quad \text{for} \quad x = 0 \qquad (2)$$

$$\Delta p_2 = 0 \quad \text{for} \quad x = x'_2 \qquad (3)$$

Sp_2 is the surface recombination velocity of the emitter.

The expression of the internal quantum efficiency in the emitter is given by:

$$\eta_{p_2} = \frac{Jp_2}{qN(1-R)} \qquad (4)$$

$$\eta_{p_2} = \frac{\alpha_2 Lp_2}{\alpha_2^2 Lp^2 - 1} \times \left\{ \frac{-\alpha_2 Lp_2 e^{-\alpha_2 x'_2} + \left(\alpha_2 Lp_2 - \frac{Sp_2 Lp_2}{Dp_2}\right) - \left[\sinh\left(\frac{x'_2}{Lp_2}\right) + \frac{Sp_2 Lp_2}{Dp_2}\cosh\left(\frac{x'_2}{Lp_2}\right)\right] e^{-\alpha_2 x'_2}}{\cosh\left(\frac{x'_2}{Lp_2}\right) + \frac{Sp_2 Lp_2}{Dp_2}\sinh\left(\frac{x'_2}{Lp_2}\right)} \right\} \qquad (5)$$

Where, Jp_2 is the photocurrent of the holes in the region 2. This equation (5) describes the contribution of the generated holes in the emitter following photon absorption.

Quantum efficiency in the space charge region

From the current and continuity equations we calculated the current density in the space charge region to deduce the expression of the internal quantum efficiency in the space charge region. The contribution of the minority carriers in the internal quantum efficiency [15] is described by equation (6):

$$\eta_{zce} = \left(1 - e^{-\alpha_2 w}\right) e^{-\alpha_2 x'_2} \qquad (6)$$

Quantum efficiency in the base

The continuity equations representing the variations of generated electrons in the base and in the substrate are given by equations (7) and (8):

$$\frac{d^2\Delta n_3}{dx^2} - \frac{\Delta n_3}{Ln_3^2} = -\frac{\alpha_3 N(1-R)e^{-(\alpha_2-\alpha_3)(x'_2+w_1)}}{Dn_3} e^{-\alpha_3 x} \qquad (7)$$

$$\frac{d^2\Delta n_4}{dx^2} - \frac{\Delta n_4}{Ln_2^2} = -\frac{\alpha_4 N(1-R)e^{-(\alpha_2-\alpha_3)(x'_2+w_1)} e^{-(\alpha_3-\alpha_4)x_3}}{Dn_4} e^{-\alpha_4 x} \qquad (8)$$

α_4 is the absorption coefficient of CdTe, Ln_4 is the diffusion length of electrons in the substrate, Dn_4 is the diffusion coefficient of electrons in the substrate.

The general solutions of equations (7) and (8) are of the type:

$$\Delta n_3(x) = A_1 e^{x/Ln_3} + B_1 e^{-x/Ln_3} + K_1 e^{-\alpha_3 x} \qquad (9)$$

$$\Delta n_4(x) = A_2 e^{x/Ln_4} + B_2 e^{-x/Ln_4} + K_2 e^{-\alpha_4 x} \qquad (10)$$

With A_1, A_2, B_1 and B_2 are constant values and K_1 and K_2 are given by:

$$K_1 = -\frac{\alpha_3 N(1-R)Ln_3^2 e^{-(\alpha_2-\alpha_3)(x'_2+w_1)}}{Dn_3(\alpha_3^2 Ln_3^2 - 1)} \qquad (11)$$

$$K_2 = -\frac{\alpha_4 N(1-R)Ln_4^2 e^{-(\alpha_2-\alpha_3)(x'_2+w_1)} e^{-(\alpha_3-\alpha_4)x_3}}{Dn_4(\alpha_4^2 Ln_4^2 - 1)} \qquad (12)$$

The constants values are determined from the boundary conditions given by equations (13 to 16) [10-12]:

$$\Delta n_3 = 0 \quad \text{for} \quad x = x'_2 + w_1 \qquad (13)$$

$$Dn_3 \frac{d\Delta n_3}{dx} = Dn_4 \frac{d\Delta n_4}{dx} \quad \text{for} \quad x = x_3 \qquad (14)$$

$$\Delta n_3 = \Delta n_4 \quad \text{for} \quad x = x_3 \qquad (15)$$

$$\Delta n_4 = 0 \quad \text{for} \quad x = H \qquad (16)$$

The internal quantum efficiency η_b describing the contribution of electron in the base is given by the result (17):

$$\eta_b = \frac{\alpha_3 Ln_3 e^{-(\alpha_2-\alpha_3)(x'_2+w_1)}}{(\alpha_3^2 Ln_3^2 - 1)} \left\{ \frac{\alpha_3 Ln_3 e^{-\alpha_3(x'_2+w)} - \left(\alpha_3 Ln_3 - \frac{Dn_3 Ln_4}{Dn_4 Ln_3}\right) + \frac{\alpha_4 Ln_4(\alpha_3^2 Ln_3^2 - 1)(1-\alpha_4 Ln_4)}{\alpha_3 Ln_3(\alpha_4^2 Ln_4^2 - 1)} e^{-\alpha_3 H}}{\cosh\left(\frac{H-(x'_2+w)}{Ln_3}\right) + \frac{Dn_4 Ln_3}{Dn_3 Ln_4}\sinh\left(\frac{H-(x'_2+w)}{Ln_3}\right)} - \frac{\left[\sinh\left(\frac{H-(x'_2+w)}{Ln_3}\right) + \frac{Dn_4 Ln_3}{Dn_3 Ln_4}\cosh\left(\frac{H-(x'_2+w)}{Ln_3}\right)\right] e^{-\alpha_3(x'_2+w)}}{\cosh\left(\frac{H-(x'_2+w)}{Ln_3}\right) + \frac{Dn_4 Ln_3}{Dn_3 Ln_4}\sinh\left(\frac{H-(x'_2+w)}{Ln_3}\right)} \right\} \qquad (17)$$

The expression of the total internal quantum efficiency resulting from the contribution of the different regions of the solar cells model is given by equation (18):

$$\eta_{total} = \eta_f + \eta_{zce} + \eta_b \qquad (18)$$

Homojunction with window and deposited on substrate CdS(N^+)/$CuInSe_2$(N)/$CuInSe_2$(P)/CdTe(P^+)

Modelling

The figures below represent the modelling of a homojonction with window layer deposited on CdTe substrate. In Fig. 4 e_1, e_2, e_3 and e_4 respectively represent the thicknesses of the window layer, the emitter, the base

and the substrate and w is the thickness of the space charge region. In Fig. 3 $x_1 = e_1$, $x_2 = e_1 + e_2$, $x_3 = e_1 + e_2 + w + e_3$ and $H = e_1 + e_2 + w + e_3 + e_4$.

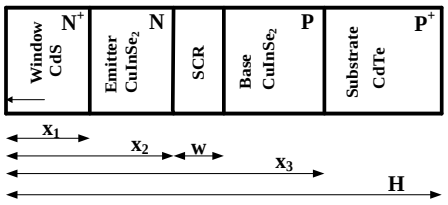

Figure 3: Diagram of structure CdS(N⁺)/CuInSe₂(N)/CuInSe₂(P)/CdTe(P⁺)

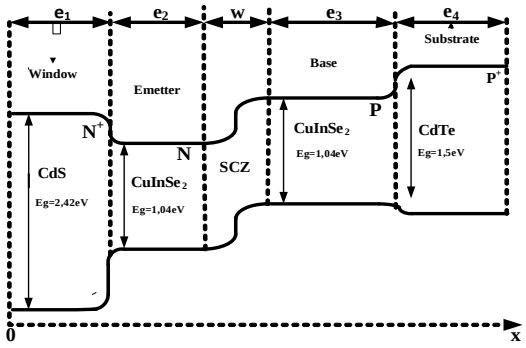

Figure 4: Energy band diagram of structure CdS(N⁺)/CuInSe₂(N)/CuInSe₂(P)/CdTe(P⁺)

Internal quantum efficiency in the window layer

The quantum efficiency in the window layer for a homojonction with window layer and deposited on substrate is the same that the emitter for the model of homojonction deposited on substrate. We have just replaced x_1, α_1, Lp_1, Dp_1 and Sp_1 respectively by x'_2, α_2, Lp_2, Dp_2 and Sp_2.

The expression of the internal quantum efficiency in the window layer becomes:

$$\eta_{p_1} = \frac{\alpha_1 Lp_1}{\left(\alpha_1^2 Lp_1^2 - 1\right)}\left\{-\alpha_1 Lp_1 e^{-\alpha_1 x_1} + \frac{\left(\alpha_1 Lp_1 - \frac{Sp_1 Lp_1}{Dp_1}\right) - e^{-\alpha_1 x_1}\left[\sinh\left(\frac{x_1}{Lp_1}\right) + \frac{Sp_1 Lp_1}{Dp_1}\cosh\left(\frac{x_1}{Lp_1}\right)\right]}{\cosh\left(\frac{x_1}{Lp_1}\right) + \frac{Sp_1 Lp_1}{Dp_1}\sinh\left(\frac{x_1}{Lp_1}\right)}\right\} \quad (19)$$

Internal quantum efficiency in the emitter

The continuity equation governing the variation of the holes in the emitter [4] is given by:

$$\frac{d^2\Delta p_2}{dx^2} - \frac{\Delta p_2}{Lp_2^2} + \frac{\alpha_2 N(1-R)e^{-(\alpha_1-\alpha_2)x_1}}{Dp_2} e^{-\alpha_2 x} = 0 \quad (20)$$

α_2 is the absorption coefficient of CuInSe₂, Lp_2 is the diffusion length of the holes in the emitter, Dp_2 diffusion coefficient of the holes in the emitter.

The general solution of equation (15) is of the type:

$$\Delta p_2(x) = A_3 e^{x/Lp_2} + B_3 e^{-x/Lp_2} + K_3 e^{-\alpha_2 x} \quad (21)$$

with A_3 et B_3 constant values and K_3 is given by

$$K_3 = -\frac{\alpha_2 N(1-R)Lp_2^2 e^{-(\alpha_1-\alpha_2)x_1}}{Dp_2(\alpha_2^2 Lp_2^2 - 1)} \quad (22)$$

The constant values are determined from the boundary conditions that are [3-6] :

$$Dp_2 \frac{d\Delta p_2}{dx} = Sp_2 \Delta p_2 + Dp_2 \frac{d\Delta p_1}{dx} \quad \text{for } x = x_1 \quad (23)$$

$$\Delta p_2 = 0 \quad \text{for } x = x_2 \quad (24)$$

Sp_2 is the recombination velocity at the window-emitter interface. The expression of the internal quantum efficiency in the emitter η_e is given by:

$$\eta_e = \left\{-\frac{\alpha_2 Lp_2 e^{-(\alpha_1-\alpha_2)x_1}}{\left(1-\alpha_2^2 Lp_2^2\right)}\left[\frac{\left(\alpha_2 Lp_2 + \frac{Sp_2 Lp_2}{Dp_2}\right)e^{-\alpha_2 x_1} - \left[\sinh\left(\frac{x_2-x_1}{Lp_2}\right) + \frac{Sp_2 Lp_2}{Dp_2}\cosh\left(\frac{x_2-x_1}{Lp_2}\right)\right]e^{-\alpha_2 x_2}}{\cosh\left(\frac{x_2-x_1}{Lp_2}\right) + \frac{Sp_2 Lp_2}{Dp_2}\sinh\left(\frac{x_2-x_1}{Lp_2}\right)} - \alpha_2 Lp_2 e^{-\alpha_2 x_2}\right]\right\} + \frac{\eta_f}{\cosh\left(\frac{x_2-x_1}{Lp_2}\right) + \frac{Sp_2 Lp_2}{Dp_2}\sinh\left(\frac{x_2-x_1}{Lp_2}\right)} \quad (25)$$

Quantum efficiency in the space charge region

The expression of the internal quantum efficiency in the space charge region is given by [15]:

$$\eta_{scr} = e^{-\alpha_1 x_1} e^{-\alpha_2 (x_2 - x_1)}\left(1 - e^{-\alpha_2 w}\right) \quad (26)$$

Quantum efficiency in the base

The continuity equations for the electron variations in the base and the substrate are given by [12]:

$$\frac{d^2\Delta n_3}{dx^2} - \frac{\Delta n_3}{Ln_3^2} = -\frac{\alpha_3 N(1-R)e^{-(\alpha_1-\alpha_2)x_1} e^{-(\alpha_2-\alpha_3)(x_2+w_1)}}{Dn_3} e^{-\alpha_3 x} \quad (27)$$

$$\frac{d^2\Delta n_4}{dx^2} - \frac{\Delta n_4}{Ln_2^2} = -\frac{\alpha_4 N(1-R)e^{-(\alpha_1-\alpha_2)x_1} e^{-(\alpha_2-\alpha_3)(x_2+w_1)} e^{-(\alpha_3-\alpha_4)x_3}}{Dn_4} e^{-\alpha_4 x} \quad (28)$$

α_4 is the absorption coefficient of the CdTe, Ln_4 is the diffusion length of the electrons in the substrate, Dn_4 diffusion coefficient of electrons in the substrate.

The general solutions of equations (23) and (24) are of the type:

$$\Delta n_3(x) = A_4 e^{x/Ln_3} + B_4 e^{-x/Ln_3} + K_4 e^{-\alpha_3 x} \quad (29)$$

$$\Delta n_4(x) = A_5 e^{x/Ln_4} + B_5 e^{-x/Ln_4} + K_5 e^{-\alpha_4 x} \quad (30)$$

With A_4, A_5, B_4 and B_5 constants and K_4, K_5 are given by:

$$K_4 = -\frac{\alpha_3 N(1-R)Ln_3^2 e^{-(\alpha_1-\alpha_2)x_1} e^{-(\alpha_2-\alpha_3)(x_2+w_1)}}{Dn_3(\alpha_3^2 Ln_3^2 - 1)} \quad (31)$$

$$K_5 = -\frac{\alpha_4 N(1-R)Ln_4^2 e^{-(\alpha_1-\alpha_2)x_1} e^{-(\alpha_2-\alpha_3)(x_2+w_1)} e^{-(\alpha_3-\alpha_4)x_3}}{Dn_4(\alpha_4^2 Ln_4^2 - 1)} \quad (32)$$

Contents lists available at http://www.jmsse.org/ & http://www.jmsse.in/

The constants are determined from the boundary conditions given by equations (25 to 28) [10-12]:

$$\Delta n_3 = 0 \quad \text{for} \quad x = x_2 + w \tag{33}$$

$$Dn_3 \frac{d\Delta n_3}{dx} = Dn_4 \frac{d\Delta n_4}{dx} \quad \text{for} \quad x = x_3 \tag{34}$$

$$\Delta n_3 = \Delta n_4 \quad \text{for} \quad x = x_3 \tag{35}$$

$$\Delta n_4 = 0 \quad \text{for} \quad x = H \tag{36}$$

The expression of the internal quantum efficiency in the base is given by:

$$\eta_b = \frac{\alpha_3 Ln_3 e^{-(\alpha_1-\alpha_2)x_1} e^{-(\alpha_2-\alpha_3)(x_2+w_1)}}{(\alpha_3^2 Ln_3^2 - 1)} \left\{ \begin{array}{l} -\alpha_3 Ln_3 e^{-\alpha_3(x_2+w)} \\ + \dfrac{\left(\alpha_3 Lp_3 - \dfrac{Ln_3 Dn_4}{Dn_3 Ln_4}\right) e^{-\alpha_3 H} + \dfrac{(\alpha_3^2 Ln_3^2 - 1)\alpha_4 Ln_4 (1-\alpha_4 Ln_4) e^{-\alpha_3 H}}{(\alpha_4^2 Ln_4^2 - 1)\alpha_3 Ln_3}}{\cosh\left(\dfrac{H-(x_2+w)}{Ln_3}\right) + \dfrac{Dn_4 Ln_3}{Dn_3 Ln_4} \sinh\left(\dfrac{H-(x_2+w)}{Ln_3}\right)} \\ + \dfrac{\left[\dfrac{Dn_4 Ln_3}{Dn_3 Ln_4} \cosh\left(\dfrac{H-(x_2+w)}{Ln_3}\right) + \sinh\left(\dfrac{H-(x_2+w)}{Ln_3}\right)\right]}{\cosh\left(\dfrac{H-(x_2+w)}{Ln_3}\right) + \dfrac{Dn_4 Ln_3}{Dn_3 Ln_4} \sinh\left(\dfrac{H-(x_2+w)}{Ln_3}\right)} e^{-\alpha_3(x_2+w)} \end{array} \right\} \tag{37}$$

The expression of the total internal quantum efficiency is given by:

$$\eta_{total} = \eta_f + \eta_{zce} + \eta_b \tag{38}$$

Homojunction deposited on substrate under the action of an additional electric field

Quantum efficiency in the emitter layer

The governing continuity equation from the variation of the holes in the N-type emitter under static mode is given by:

$$\frac{d^2\Delta p_2}{dx^2} - \frac{\mu p_2 E}{Dp_2}\frac{d\Delta p_2}{dx} - \frac{\Delta p_2}{Lp_2^2} + \frac{\alpha_2 \cdot N(1-R)e^{-\alpha_2 x}}{Dp_2} = 0 \tag{39}$$

The general solution of equation (31) is given by:

$$\Delta p_2(x) = A_6 e^{r_1 x} + B_6 e^{r_2 x} + K_6 e^{-\alpha_2 x} \tag{40}$$

With

$$\left\{ \begin{array}{l} r_1 = \dfrac{\mu_{p2} E}{2Dp_2} + \sqrt{\left(\dfrac{\mu_{p2} E}{2Dp_2}\right)^2 + \left(\dfrac{1}{Lp_2}\right)^2} \\ r_2 = \dfrac{\mu_{p2} E}{2Dp_2} - \sqrt{\left(\dfrac{\mu_{p2} E}{2Dp_2}\right)^2 + \left(\dfrac{1}{Lp_2}\right)^2} \end{array} \right.$$

The constants A_6 and B_6 are determined from the boundary conditions given by equations (41) and (42)

$$Dp_2 \frac{d\Delta p_2}{dx} - \mu_{p2} . E . \Delta p_2 = Sp_2 \cdot \Delta p_2 \quad \text{for } x = 0 \tag{41}$$

$$\Delta p_2 = 0 \quad \text{for } x = x' \tag{42}$$

The photocurrent in the emitter is given by:

$$J_{f2} = -qDp_2 \frac{d\Delta p_2}{dx} \quad \text{for} \quad x = x'_2 \tag{43}$$

It becomes:

$$J_{f2} = \frac{q\alpha_2 N(1-R)L'}{\left(\alpha_2 + \frac{1}{l}\right)^2 L'^2 - 1} \left\{ \begin{array}{l} -\alpha_2 L' e^{-\alpha_2 x'_2} + \dfrac{e^{\frac{x'_2}{l}}\left(\alpha_2 L' + \frac{Sp_2 L'}{Dp_2} + \frac{2L'}{l}\right)}{\cosh\left(\frac{x'_2}{L'}\right) + \left(\frac{Sp_2 L'}{Dp_2} + \frac{L'}{l}\right)\sinh\left(\frac{x'_2}{L'}\right)} \\ - \dfrac{e^{-\alpha_2 x'_2}\left[\left(\frac{Sp_2 L'}{Dp_2} + \frac{2L'}{l}\right)\cosh\left(\frac{x'_2}{L'}\right) + \left(\frac{Sp_2 L'^2}{Dp_2 l} + \frac{L'^2}{l^2} + 1\right)\sinh\left(\frac{x'_2}{L'}\right)\right]}{\cosh\left(\frac{x'_2}{L'}\right) + \left(\frac{Sp_2 L'}{Dp_2} + \frac{L'}{l}\right)\sinh\left(\frac{x'_2}{L'}\right)} \end{array} \right\} \tag{44}$$

With $l = \dfrac{2Dp_2}{\mu_{p2} . E}$ and $L' = \dfrac{l . Lp_2}{\sqrt{(Lp_2^2 + l^2)}}$

The expression of the internal quantum efficiency in the emitter is [16]:

$$\eta_{f2} = \frac{J_{f2}}{qN(1-R)} \tag{45}$$

$$\eta_{f2} = \frac{\alpha_2 L'}{\left(\alpha_2 + \frac{1}{l}\right)^2 L'^2 - 1} \left\{ \begin{array}{l} -\alpha_2 L' e^{-\alpha_2 x'_2} + \dfrac{e^{\frac{x'_2}{l}}\left(\alpha_2 L' + \frac{Sp_2 L'}{Dp_2} + \frac{2L'}{l}\right)}{\cosh\left(\frac{x'_2}{L'}\right) + \left(\frac{Sp_2 L'}{Dp_2} + \frac{L'}{l}\right)\sinh\left(\frac{x'_2}{L'}\right)} \\ - \dfrac{e^{-\alpha_2 x'_2}\left[\left(\frac{Sp_2 L'}{Dp_2} + \frac{2L'}{l}\right)\cosh\left(\frac{x'_2}{L'}\right) + \left(\frac{Sp_2 L'^2}{Dp_2 l} + \frac{L'^2}{l^2} + 1\right)\sinh\left(\frac{x'_2}{L'}\right)\right]}{\cosh\left(\frac{x'_2}{L'}\right) + \left(\frac{Sp_2 L'}{Dp_2} + \frac{L'}{l}\right)\sinh\left(\frac{x'_2}{L'}\right)} \end{array} \right\} \tag{46}$$

The expression of the quantum efficiency in the space charge region and in the base remains the same that the homojunction with window layer and deposited by substrate.

Homojunction with window layer deposited on substrate under the action of an additional electric field

Quantum efficiency in the emitter layer

The quantum efficiency in the window layer for a homojunction with window layer deposited on substrate with the presence of an additional electric field is the same that the emitter for the model of homojunction deposited on substrate in the presence of an additional electric field. We have just replaced x'_2, α_2, Lp_2, Dp_2, μp_2 and Sp_2 respectively by x_1, α_1, Lp_1, Dp_1, μp_1 and Sp_1. Thus the expression of the internal quantum efficiency in the window layer becomes:

$$\eta_{f1} = \frac{\alpha_1 L'}{\left(\alpha_1 + \frac{1}{l}\right)^2 L'^2 - 1} \left\{ \begin{array}{l} -\alpha_1 L' e^{-\alpha_1 x_1} + \dfrac{e^{\frac{x_1}{l}}\left(\alpha_1 L' + \frac{Sp_1 L'}{Dp_1} + \frac{2L'}{l}\right)}{\cosh\left(\frac{x_1}{L'}\right) + \left(\frac{Sp_1 L'}{Dp_1} + \frac{L'}{l}\right)\sinh\left(\frac{x_1}{L'}\right)} \\ - \dfrac{e^{-\alpha_1 x_1}\left[\left(\frac{Sp_1 L'}{Dp_1} + \frac{2L'}{l}\right)\cosh\left(\frac{x_1}{L'}\right) + \left(\frac{Sp_1 L'^2}{Dp_1 l} + \frac{L'^2}{l^2} + 1\right)\sinh\left(\frac{x_1}{L'}\right)\right]}{\cosh\left(\frac{x_1}{L'}\right) + \left(\frac{Sp_1 L'}{Dp_1} + \frac{L'}{l}\right)\sinh\left(\frac{x_1}{L'}\right)} \end{array} \right\} \tag{47}$$

The expression of the quantum efficiency in the emitter, in the space charge region and in the base remains the same in the case of homojunction with window layer and deposited on substrate.

Results and Discussion

Absorption coefficients of the different materials used

For each structure, a theoretical model is proposed to determine the internal quantum efficiency. The variation of absorption coefficients of the materials ($CuInSe_2$, CdS and CdTe) is given according to the energy by the Fig. 1 [2]. However, we note for some values of energy (1.04eV, 1.5eV and 2.3eV) corresponding respectively to each material, an abrupt increase of the absorption coefficients up to a certain value (10^5 cm^{-1}) where an increase is observed. Indeed, these energy values correspond respectively to the gaps of these materials. For each material, we note an abrupt absorption.

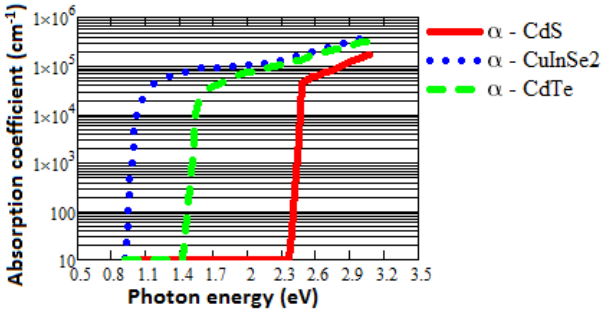

Figure 5: Evolution curve of the absorption coefficient as a function of energy

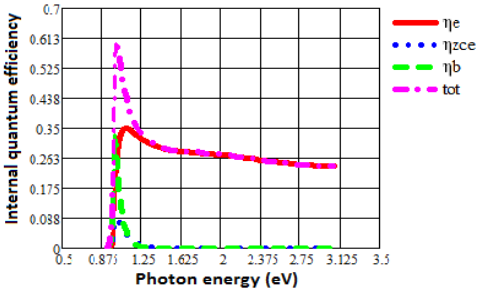

Figure 6 : Contribution of the quantum efficiency of a homojunction deposited by substrate, (x'_2 =0.5µm, Lp_2=0.5 µm, Sp_2=2.$10^5$$cms^{-1}$, Dp_2=20cm^2s^{-1}, w=0.2µm, w_1=0.1µm, Ln_3=3 µm, Ln_4=3 µm, Sn_3=2.$10^6$$cms^{-1}$, Dn_3=20cm^2s^{-1}, H=8µm)

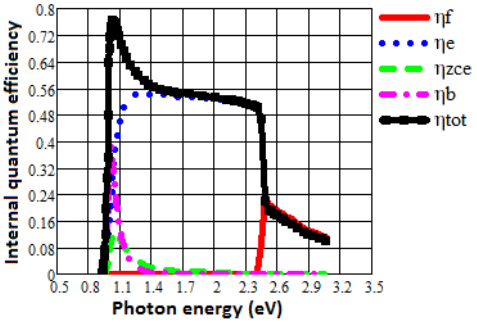

Figure 7 : Comparison of the different regions of the cell for a homojunction with window layer and deposited by substrate (x_1=0.5µm, x_2=1µm, Lp_1=0.5µm, Sp_1=2.$10^6$$cms^{-1}$, Dp_1=20cm^2s^{-1}, Lp_2=0.5µm, Sp_2=2.$10^5$$cms^{-1}$, Dp_2=20cm^2s^{-1} w=0.2µm, w_1=0.1µm, Ln_3=3 µm, Ln_4=3 µm, Sn_3=2.$10^6$$cms^{-1}$, Dn_3=20cm^2s^{-1}, H=4.2µm, H_b=H-(x_2+w))

Contribution in quantum efficiency of the different regions of a homojunction deposited by substrate with or without a window layer: CdS(N^+)/$CuInSe_2$(N)/ $CuInSe_2$(P)/CdTe(P^+) et $CuInSe_2$ (N)/$CuInSe_2$(P)/CdTe(P^+)

Figures 6 and 7 show the contribution in internal quantum efficiency of the different regions of the homojunction deposited on substrate with or without a window layer as well as the total quantum efficiency of the cell.

The analysis of the spectral response shows that the three regions (emitter, space charge region and base) practically absorb for the same energy. This is due to the fact that it concerns a homojunction model. The window layer absorbs for an energy substantially equal to 2.5eV [17]. However, the contribution to the photocurrents of the base and the emitter remains higher than the photocurrent of space charge region [18]. This is related to the low value of the space charge region thickness resulting in a weak generation of minority carriers in this region. We note that for photon energies higher than 1.2eV, only the generated minority carriers in the emitter contribute to the signal. This observation is due to the fact that for energies higher than 1.2eV all the transmitted photon flux is absorbed in the emitter consequently only the generated holes in the emitter contribute to the photocurrent. The total quantum efficiency is maximum for a photon energy of the order of 1.1eV corresponding to the gap of the $CuInSe_2$ material. The decrease of the spectral response just after the maximum can be attributed to the phenomena of surface recombination.

Comparison of different models

Contribution in quantum efficiency in the emitter of the different cells

In this part, the study of the spectral response of the solar cells of the different models in report to the energy was made in Fig. 8 below.

In this figure, we see a clear improvement of the quantum efficiency of the emitter for a homojunction with window layer and deposited on substrate. This contribution is due to the reduction of surface losses [13]. For the homojunction deposited on substrate, its efficiency is considerably lower compared to the homojunction with a window layer and deposited by substrate. For the photon energies between 0.92eV and 1.18eV, the absorption of $CuInSe_2$ generates holes and electrons that will be collected if their diffusion lengths are sufficient. We thus obtain a theoretical efficiency of 54.3% for collected carriers. For energies between 1.18eV and 2.48eV we note a decrease in quantum efficiency due to the absorption decrease of $CuInSe_2$ and the surface recombination velocity. From 2.48eV, the CdS starts to absorb and we observe a decrease of the quantum efficiency which is due to the low diffusion lengths and the surface losses [19].

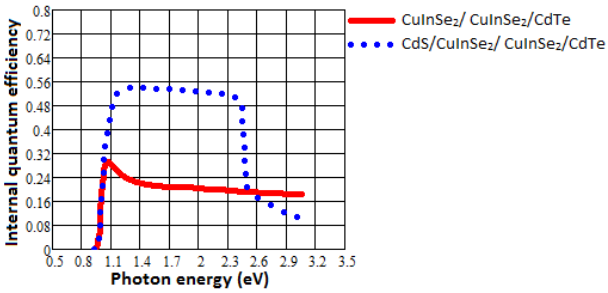

Figure 8 : Contribution of the quantum efficiency of the emitter (x_1=0.5µm, x_2=1µm, Lp_1=0.5µm, Sp_1=2.$10^6$$cm^2s^{-1}$, Dp_1=20cm^2s^{-1}, Lp_2=0.5 µm, Sp_2=2.$10^5$$cms^{-1}$)

Contribution of quantum efficiency in the space charge region of different cells

Figure 9 shows the contribution of the quantum efficiency of the two models in the space charge region. In this region, we observe that the contribution of the quantum efficiency of the homojunction with window layer and deposited by substrate is greater than that of the homojunction deposited by substrate.

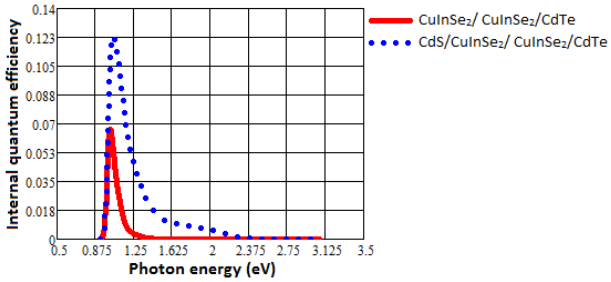

Figure 9: Comparison of the contribution of the quantum efficiency of the space charge region of the different cells (x_1=0.5µm, x_2=1µm, x'_2=x_1-x_2=0.5µm, w=0.2µm, w_1=0.1 µm)

Contribution of the quantum efficiency in the base of the different cells

Figure 10 represents the contribution of the quantum efficiency of the two models in the base. In this figure we see that the quantum efficiency of the homojunction with window layer and deposited by substrate is greater than that of the homojunction deposited by substrate. In this case we can say that it is the effect of the substrate which is at the origin of this difference.

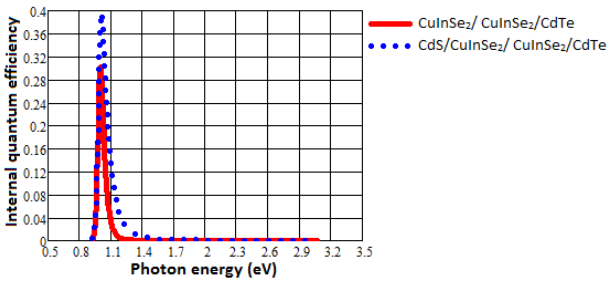

Figure 10: Comparison of the contribution of the quantum efficiency of the base of the different models (x_1=0.5µm, x_2=1µm, Lp_1=0.5 µm, Sp_1=2.10^{6}cms^{-1}, Dp_1=20cm^{2}s^{-1}, Lp_2=0.5µm, Sp_2=2.10^{5}cms^{-1}, Dp_2=20cm^{2}s^{-1} w=0.2µm, w_1=0.1µm, Ln_3=3 µm, Ln_4=3 µm, Sn_3=2.10^{6}cms^{-1}, Dn_3=20cm^{2}s^{-1}, H=4.2µm, H_b=H-(x2+w)=3 µm)

Efficiency of the different cells

The contribution of the different regions of each model allowed us to do a comparative study of these different devices. From these studies we can predict that homojunction with window layer and deposited by substrate will give the best quantum efficiency.

The figure below (Fig. 11) represents the variation of the total quantum efficiency of the two models (CdS (N^+) / $CuInSe_2$ (N) / $CuInSe_2$ (P) / CdTe (P^+) and$CuInSe_2$ (N) / $CuInSe_2$ (P) / CdTe (P^+)). The energy photons higher than the gap energy of $CuInSe_2$ create charge carriers that will be collected under the effect of an internal electric field if they reach the space charge region. That is what explains the increase in quantum efficiency for energies between 0.92eV and 1.03eV. Some of these photocarriers created far from the space charge region will not contribute to the photocurrent if they do not have sufficient diffusion lengths. These carriers recombine hence the decrease in quantum efficiency for energies greater than 1.03eV. The best quantum efficiency (74.9%) is obtained with the homojunction model with window layer and deposited by substrate CdS (N^+) / $CuInSe_2$ (N) / $CuInSe_2$ (P) / CdTe (P^+). For the homojunction deposited on substrate without window, we have an efficiency which is of the order of 54.9%. The homojunction model with window layer and deposited by substrate combines the advantages of the window layer and the substrate. The window layer enables to reduce the losses on the surface of the emitter [2] and the substrate enables to create a rear field that pushes the carriers that normally were not collected towards the space charge region so that they can participate in the photocurrent [11].

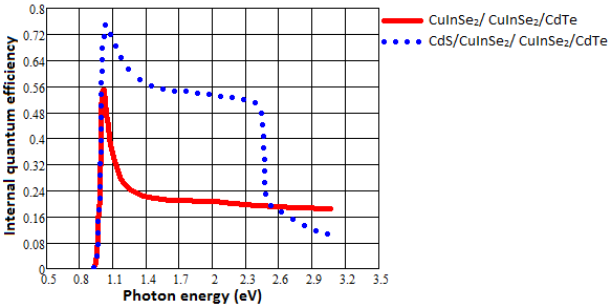

Figure 11 : Comparison of the contribution of the total quantum efficiency of the different models (x_1=0.5µm, x_2=1µm, x_2'=0.5µm, Lp_1=0.5 µm, Sp_1=2.10^{6}cms^{-1}, Dp_1=20cm^{2}s^{-1}, Lp_2=0.5µm, Sp_2=2.10^{5}cms^{-1},Dp_2=20cm^{2}s^{-1} w=0.2µm, w_1=0.1µm, Ln_3=3 µm, Ln_4=3 µm, Sn_3=2.10^{6}cms^{-1}, Dn_3=20cm^{2}s^{-1}, H=4.2µm, H_b=H-(x_2+w)=3 µm)

Effect of an additional electric field in the emitter on homojunction deposited on substrate

The losses due to the recombination in volume and surface are reduced by improving the quality of the material and by reducing the thickness and the recombination velocity of the emitter [15]. Alway sin improving the internal quantum efficiency of a solar cell, an electric field can be created in the emitter for a homojunction deposited by substrate without window layer $CuInSe_2$(N)/$CuInSe_2$(P)/CdTe(P^+).

FIG. 12 represents the variation of the internal quantum efficiency as a function of the energy of the incident photons for different values of the additional electric field. In this figure we find that for an electric field between 0 and 2000V/cm the quantum efficiency remains almost invariant. Despite the invariant of quantum efficiency, it remains almost equal to the quantum efficiency of the homojunction with window layer and deposited by substrate without an electric field. For values of the electric field greater than 2000V/cm the quantum efficiency increases with the increase of the electric field. This increase can be justified by the fact that the electric field increases the velocity of the charge carriers whose diffusion lengths were insufficient. These charge carriers will arrive at the space charge region and will be collected. We can say that the more the electric field is intense, the more the carriers will be collected and the efficiency increases.

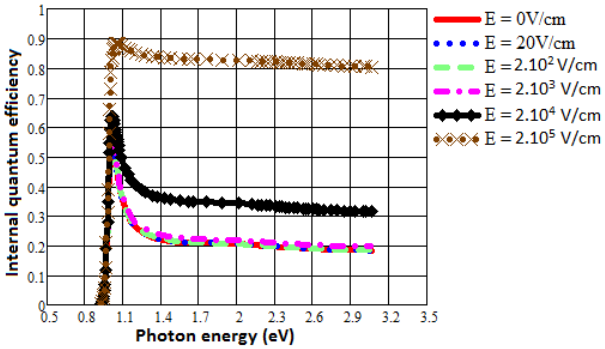

Figure 12 : Quantum efficiency of a homojunction for different values of an additional electric field (x_1=0.5µm, x_2=1µm, x_2'=0.5µm, Lp_1=0.5 µm, Sp_1=2.10^{6}cms^{-1} , $Dp1$=20cm^{2}s^{-1}, $Lp2$=0.5µm, Sp_2=2.10^{5}cms^{-1}, Dp_2=20cm^{2}s^{-1}, w=0.2µm, w_1=0.1µm, Ln_3=3µm, Ln_4=3µm, Sn_3=2.10^{6}cms^{-1}, Dn_3=20cm^{2}s^{-1}, H=4.2µm, Hb = H-(x2+w)=3 µm, μp_2=50 cm^{2}V^{-1}s^{-1})

Effect of an additional electric field in the window layer on a homojunction with a window layer and deposited on substrate

The losses due to the recombination in volume and surface are reduced by improving the quality of the material and decreasing the thickness and recombination velocity of the window layer [15]. Always in the improvement of the internal quantum efficiency of a solar cell, an electric field can be created in the window layer for a homojunction with a window layer and deposited by $CuInSe_2$(N)/$CuInSe_2$(P)/CdTe(P$^+$) substrate. Figure 13 represents the variation of the internal quantum efficiency as a function of the energy of the incident photons for different values of the additional electric field. In this figure, we remark that for an electric field between 0 and 2000Vcm^{-1} the quantum efficiency remains almost invariant. Despite the invariance of quantum efficiency, it remains almost equal to the quantum efficiency of the homojunction with window layer and deposited by substrate without an electric field. For electric field values greater than 2000Vcm^{-1} the quantum efficiency increases with the growth of the electric field. This can be justified by the fact that the electric field increases the velocity of the less hot charge carriers allowing them to reach the space charge region in order to be collected. This increase occurred at energies above 2.4 eV.

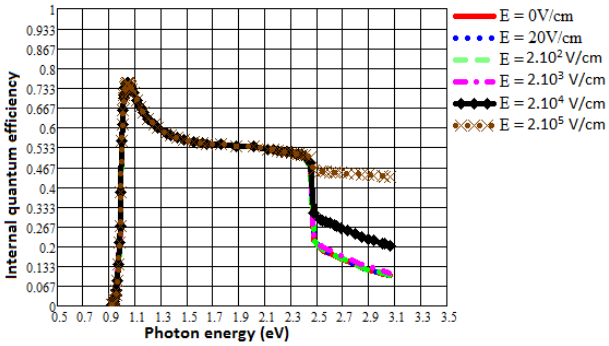

Figure 13 : Quantum efficiency of a homojunction for different values of an additional electric field (x_1=0.5µm, x_2=1µm, x_2'=0.5µm, Lp_1=0.5 µm, Sp_1=2.10^{6}cms^{-1} , $Dp1$=20cm^2 s^{-1}, $Lp2$=0.5µm, Sp_2=2.10^{5}cms^{-1}, Dp_2=20cm^{2}s^{-1}, w=0.2µm, w_1=0.1µm, Ln_3=3µm, Ln_4=3µm, Sn_3=2.10^{6}cms^{-1}, Dn_3=20cm^{2}s^{-1}, H=4.2µm, Hb = H-(x2+w)=3 µm, μp_2=50 cm^{2}V^{-1}s^{-1}))

Comparison between a homojunction deposited on substrate with or without window layer in the presence of an additional electric field 2.10^5 V/cm.

The figure below (FIG. 14) represents the comparison of the variation of the total quantum efficiency of the two models CdS(N$^+$)/$CuInSe_2$(N)/$CuInSe_2$ (P)/CdTe (P$^+$) and $CuInSe_2$ (N)/$CuInSe_2$ (P)/CdTe (P$^+$)) in presence of an additional electric field.

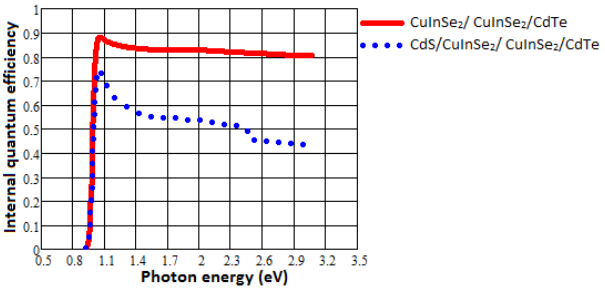

Figure 14 : Quantum efficiency of a homojunction for different values of an additional electric field (x_1=0.5µm, x_2=1µm, x_2'=0.5µm, Lp_1=0.5 µm, Sp_1=2.10^{6}cms^{-1} , $Dp1$=20cm^2 s^{-1} , $Lp2$=0.5µm, Sp_2=2.10^5 cms^{-1}, Dp_2=20cm^2 s^{-1}, w=0.2µm, w_1=0.1µm, Ln_3=3µm, Ln_4=3µm, Sn_3=2.10^{6}cm s^{-1}, Dn_3=20cm^2 s^{-1}, H=4.2µm, Hb = H-(x2+w)=3 µm, μp_2=50 cm^{2}V^{-1}s^{-1})

The best quantum efficiency (88.2%) is obtained with the model of homojunction deposited on substrate in the presence of an additional electric field. For homojunction with window layer and deposited on substrate we have an efficiency which is in the order of 74.9%. This can be explained by the fact that the emitter of the homojunction deposited on substrate has a small thickness and the additional electric field acts on the photons with energies higher than 0.924eV. While for homojonction with window layer and deposited on substrate, the additional electric field acts on photons with energies higher than 2,4eV.

Conclusions

The comparative study of the two models allowed us to conclude that the homojontion with window layer and deposited on substrate represents the best model with an internal quantum efficiency of 74.9%. The improvement observed is simply caused by the reduction of losses on the surface but also by the recovery of some electrons in the base normally lost. This performance is obtained by using the same geometrical parameters for the two studied models. This study showed us that the effect of the window layer dominates that of the substrate. It is important to choose a window layer and a substrate whose mesh parameters are similar to the base material ($CuInSe_2$) to reduce losses at the interface. The quantum efficiency improvement can also be done by creating an additional electric field. This field is created in the window layer and in the emitter respectively for a homojontion deposited on substrate with or without a window layer. This field accelerates slow carriers and is created by a doping gradient. The comparison allowed us to conclude that the homojontion deposited on substrate represents the best model with an internal quantum efficiency of 88.2% for an additional electric field of 2.10^5 Vcm^{-1}.

References

1. S. Khelifi et A. Belghachi "Rôle de la couche fenêtre dans les performances d'une cellule solaire GaAs" Rev. Energ. Ren. 7, 2004, 13-21.

2. L.S. Hamideche, A. Amara, M. Mekhnache, O. Kamli, A. Benaldjia, A. Drici, J.C. Bernede, M. Guerioune, N. Benslim, L. Bechiri, Nanostructured thermally evaporated $CuInSe_2$ thin films synthesized from mechanically alloyed powders and self-combustion ingot, Mater. Sci. Semicond. Proc. 15**,** 2012, 145–151.
3. B. Mbow, A. Mezerreg, N. Rezzoug and C. Linare, Calculed and measure spectral response in near-infrarouge of III-V photo detectors based on Ga, In and Sb, Physica Status Solidi (a) 1994, 513-524.
4. E. M. Keita, B. Mbow, M.S. Mane, M. L. Sow, C. Sow, C. Sene, Theoretical study of spectral responses of homojonctions^{2}2z based on $CuInSe_2$, Journal of Materials Science & Surface Engineering, 4(4), 2016, 392-399.
5. C.J. Huang et al., Formation of $CuInSe_2$ thin films on flexible substrates by electrodeposition (ED) technique, Solar Energy Materials & Solar Cells, 82, 2004, 553–565.
6. O. Meglali et al., Characterization of $CuInSe_2$ thin films elaborated by electrochemical deposition, Revue des Energies Renouvelables, 11 (1), 2008, 19 – 24.
7. B. Eisener, M. Wagner, D. Wolf, G. Muller, Study of the intrinsic defects in solution grown $CuInSe_2$ crystals depending on the path of crystallization, J. Cryst Growth, 198-199, 1999, 321.
8. A. Duchatelet, Synthèse de couches minces de Cu (In, Ga) Se2 pour cellules solaires, par électro-dépôt d'oxydes mixtes de cuivre-indium-gallium, Thèse de doctorat. Universite Lille1 (France), 2012, 22.
9. T. Wada, H. Kinoshita, Preparation of $CuIn(S,Se)_2$ by mechanochemical process» Thin Solid Films, 480-481 ,2005, 92-94.
10. B.M.D. Lai, Modélisation et simulation d'une cellule solaire en couche mince à base de di séléniure de Cuivre, d'Indium et de Gallium CIGS, Mémoire de Master professionnel. Université Kasdi Merbah–Ouargla 2012.
11. E.M. Keita, B. Mbow, M.L. Sow, C. Sow, M. Thiam, Theoretical comparative study of internal quantum efficiency of thin films solar cells based on $CuInSe_2$: $P^+/P/N/N^+$, $P/N/N^+$, $P^+/P/N$ And P/N models, International Journal of Engineering science & Research Technology, 5(9), 2016, 347-399.
12. A. Laugier U. A. Roger, Les photopiles solaires, technique et documentation, Ed 1981.
13. S. Madougou, F. Made, M. Boukary and G. Sissoko, Recombination parameters determination by using Internal Quantum Efficiency (IQE) data on bifacial silicon solar cells, Advanced Materials Research, 18-19, 2007, 314.
14. Y. SAYAD, Détermination de la longueur de diffusion des porteurs de charges minoritaires dans le silicium cristallin par interaction lumière-matière, Thèse de doctorat. Université de Mentouri Constantine (Algerie), 2009, 24.
15. C. Sow, B. Mbow, Y. Tabar, B. Ndiaye, M. Thiam, E.M. Keita, Theoretical study of internal quantum efficiency based on homojonction $CuInSe_2$ (n/p) with CdS window grown on CdTe substrate, International Journal of Engineering science & Research Technology, 6(1), 2017, 140-153.
16. C. Touzi, Z. Chine, T. Boufaden, B. El Jani , Etude de la reponse spectrale des cellules photovoltaiques a base de GaN, Phys. Chem. News 1, 2001, 69-72.
17. O.A. Niass, B. Mbengue, B. Ba, A. Ndiaye et I. Youm, Effet des excitons sur le rendement quantique de la cellule solaire CdS/CdTe par le modèle de la fonction diélectrique, Revue des Energies Renouvelables, 12 (3) , 2009, 503.
18. N. Touafek, M.S. Aida, R. Mahamdi, $CuInSe_2$ Solar cells Efficiency optimization, America Journal of Materials Science, 2012, 2(5), 160-164.
19. A. Kaminski, M. Monville cours, Energie photovoltaïque : Physique des composants nanostructures, INP Grenoble - INSA Lyon Solarforce PHELMA-Septembre, 2010, 22.